ACADEMIC PRESS

Available online at www.sciencedirect.com
SCIENCE DIRECT®

Journal of Colloid and Interface Science 266 (2003) 120–126

JOURNAL OF Colloid and Interface Science

www.elsevier.com/locate/jcis

Estimation of zeta potential by electrokinetic analysis of ionic fluid flows through a divergent microchannel

Myung-Suk Chun,[a,*] Sang-Yup Lee,[a,1] and Seung-Man Yang [b]

[a] *Complex Fluids and Membrane Team, Korea Institute of Science and Technology (KIST), P.O. Box 131, Cheongryang, Seoul 130-650, South Korea*
[b] *Department of Chemical and Biomolecular Engineering, Korea Advanced Institute of Science and Technology (KAIST), 373-1, Kusung-Dong, Yusung-Ku, Taejon 305-701, South Korea*

Received 15 November 2002; accepted 22 May 2003

Abstract

The streaming potential is generated by the electrokinetic flow effect within the electrical double layer of a charged solid surface. Surface charge properties are commonly quantified in terms of the zeta potential obtained by computation with the Helmholtz–Smoluchowski (H–S) equation following experimental measurement of streaming potential. In order to estimate a rigorous zeta potential for cone-shaped microchannel, the correct H–S equation is derived by applying the Debye–Hückel approximation and the fluid velocity of diverging flow on the specified position. The present computation provides a correction ratio relative to the H–S equation for straight cylindrical channel and enables us to interpret the effects of the channel geometry and the electrostatic interaction. The correction ratio decreases with increasing of diverging angle, which implies that smaller zeta potential is generated for larger diverging angle. The increase of Debye length also reduces the correction ratio due to the overlapping of the Debye length inside of the channel. It is evident that as the diverging angle of the channel goes to nearly zero, the correction ratio converges to the previous results for straight cylindrical channel.
© 2003 Elsevier Inc. All rights reserved.

Keywords: Helmholtz–Smoluchowski equation; Electrokinetic flow; Zeta potential; Streaming potential; Linearized Poisson–Boltzmann equation; Divergent microchannel

1. Introduction

When the ionized fluid is forced to flow through a charged microchannel under the pressure gradient, the counterions in the diffuse layer of the electric double layer are carried toward the downstream end. As a result, the streaming current is induced in the pressure-driven flow direction, and the electrokinetic streaming potential is generated. The streaming potential also acts to build up the conduction current in the direction opposite to the streaming current. In a steady Poiseuille flow through a capillary channel, a relation between the ratio of streaming potential difference ΔE to pressure gradient ΔP and the zeta potential ζ is described by the well-known Helmholtz–Smoluchowski (H–S) equation [1] as

$$\frac{\Delta E}{\Delta P} = \frac{\varepsilon\zeta}{\mu\left(\lambda_0 + \frac{\lambda_s}{R}\right)}, \tag{1}$$

where λ_0 is the electrolyte conductivity, λ_s the specific surface conductivity, ε the dielectric constant, μ the viscosity of electrolyte solution, and R the capillary radius. Suppose that the dielectric constant of the liquid phase is much larger than that in the solid phase.

Earlier studies have been performed to examine the electrokinetic flow in capillaries, where the H–S equation has been derived under the condition that the Debye length κ^{-1} is small compared to the capillary radius R. Rice and Whitehead [2] presented the effect of the surface potential on fluid transport through narrow cylindrical capillary, where the Debye–Hückel (D–H) approximation was applied for arbitrary values of κR. Extending this approach, Levine et al. [3] addressed the analytical solutions of the Poisson–Boltzmann (P–B) equation for symmetric monovalent electrolytes with a wide range of surface poten-

* Corresponding author.
E-mail address: mschun@kist.re.kr (M.-S. Chun).
[1] Current address: School of Chemical Engineering, Purdue University, West Lafayette, IN 47907, USA.

0021-9797/$ – see front matter © 2003 Elsevier Inc. All rights reserved.
doi:10.1016/S0021-9797(03)00576-9

tials. Since the late 1980s, numerous membrane science researchers have investigated the determination of membrane electrokinetic properties utilizing the H–S equation, with the results being expressed in terms of membrane zeta potential [4–10]. Based on the previous approach of Levine et al. [3], a solution of the nonlinear P–B equation for a cylindrical pore coupled with a solution for electrokinetic effects for symmetric electrolytes was computed by Bowen and Cao [11]. Their result of the correction factor depending on the κR shows that the use of classical analysis is likely to lead to substantial underestimation of the true zeta potential. Szymczyk et al. [12] established a global streaming potential formula for two-layer asymmetric pore consisting of skin and support layer, and evaluated the relative contribution of each layer upon the electrokinetic properties.

It should be recognized that, in most of the relevant studies, the zeta potential has been determined by applying the H–S equation derived from the straight cylindrical channel. The fact that the electrokinetic flow property is changed by the variations of the geometry of channel means a requirement for the derivation of correct H–S equation so as to estimate a more rigorous value of zeta potential. However, this problem is nontrivial and the analysis becomes much more difficult [13,14]. The flow geometry of practical interest considered in the present study is the divergent channel. This geometry is frequently encountered many microsystems, such as several kinds of narrow channels formed in the microfluidic devices, microcapillary electrophoresis, and microbiochips [15,16]. Both diverging and converging flows are efficiently applied to drive the microscale flow control. Although it is not readily available, the cone-shaped channel can also be found in the pore structure of membranes or filters. For example, the structure of anodized anisotropic aluminum membrane that is used in ultrafiltration and microfiltration exhibits a cone-shaped divergent channel. In this, the topological observations of anisotropic membrane pores display a character of pore (or void) size gradients; the membrane anisotropy is produced by a controlled variation of current density during the pore growth [17]. The pores in the top skin layer and the quasicircular void in the bottom surface of the support layer correspond to an inlet and an outlet of the channels, respectively.

In the present study, the correct H–S equation applied for the cone-shaped channel is developed to obtain a rigorous zeta potential. The velocity field with diverging flow is analyzed by using the streaming function, and then the electrostatic potential is favorably considered based on the D–H approximation. We investigate the variation of the correction to the original H–S equation for cylindrical channels with various diverging angles as well as the relative Debye lengths. The present study extends the classical H–S principle to a cone-shaped microchannel with the practical motivation.

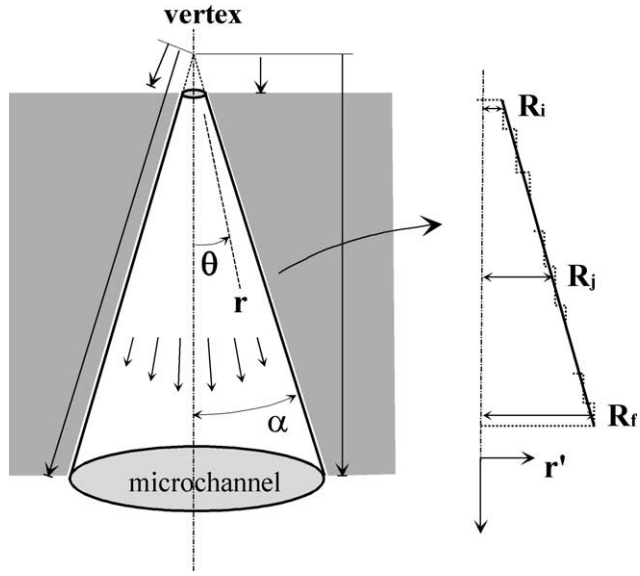

Fig. 1. Schematic illustration of diverging flow through a cone-shaped microchannel, where the cone geometry is approximated as an assemblage of finite number of straight unit cylinders with radius R_j for the calculation of streaming current.

2. Diverging flow through a cone-shaped microchannel

We begin by considering the flow geometry that is depicted in Fig. 1. For convenience, we take the spherical polar coordinates for steady state, fully developed flow. In Fig. 1, α indicates the diverging angle of cone-shaped microchannel, and both radial distance and polar angle in spherical coordinates are noted as r and θ, respectively. Due to the axisymmetry of the geometry, the velocity profile v and the pressure P in diverging flow can be obtained by the use of stream function defined in cone-shaped geometry [18].

The velocity profile of the axisymmetric creeping flow is independent of the azimuthal angle in the cone-shaped microchannel. The streamlines are obviously straight lines radiating from the vertex of the cone and given by the values $\theta =$ constant. Therefore, the stream function must be independent of r (i.e., $\Phi = \Phi(\theta)$), that is equivalent to $v_\varphi = v_\theta = 0$. Applying the Gegenbauer functions in combination with Legendre functions provides the general solution for the stream function in spherical coordinates [19]. The stream function is zero along the axis of the channel and the no-slip boundary condition is required at the channel wall. Given volumetric flow rate through the channel in the z direction, q, the radial velocity is obtained as

$$v(r,\theta) = v_r = \frac{3q}{2\pi r^2}\frac{\cos^2\theta - \cos^2\alpha}{(1+2\cos\alpha)(1-\cos\alpha)^2}. \tag{2}$$

Since $q = \pi(r\sin\alpha)^2\langle v_r\rangle$, Eq. (2) becomes

$$v_r = \langle v_r\rangle\frac{3\sin^2\alpha}{2}\frac{\cos^2\theta - \cos^2\alpha}{(1+2\cos\alpha)(1-\cos\alpha)^2}. \tag{3}$$

As the diverging angle α goes to zero, Eq. (3) converges to a Poiseuille flow pattern. At any point in the channel space, the

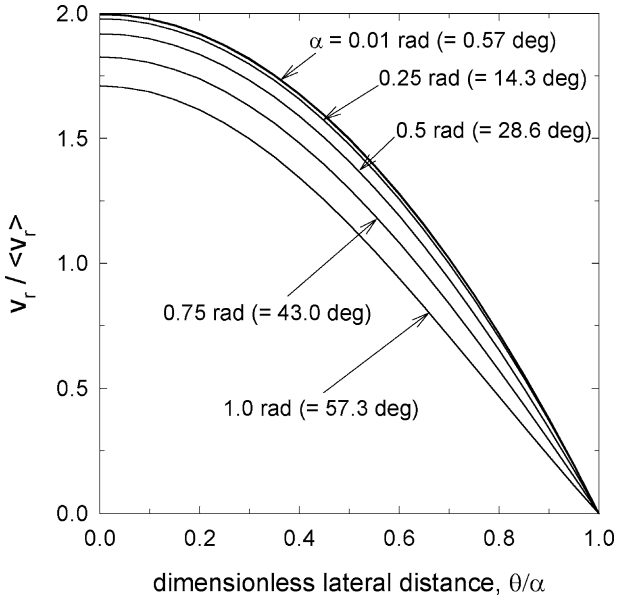

Fig. 2. The variation of the dimensionless radial velocity profile in a cone-shaped channel with different diverging angles α.

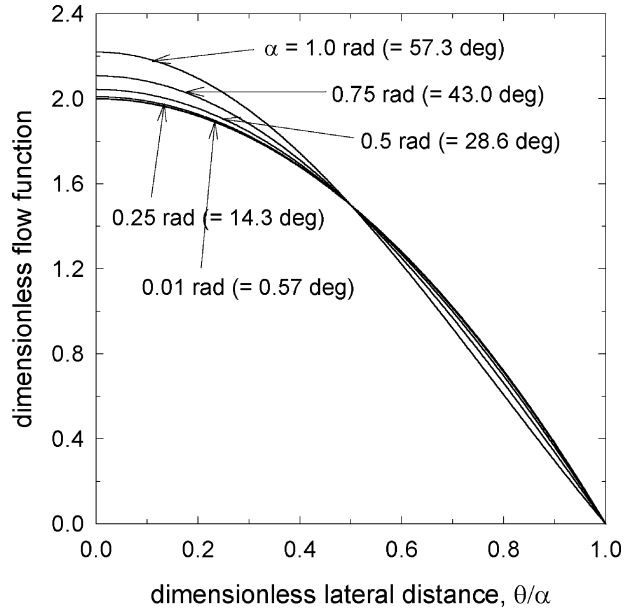

Fig. 3. The variation of the dimensionless flow function in a cone-shaped channel with different diverging angles α.

cylindrical coordinates can be generated from the relations as $r^2 = r'^2 + z^2$ and $\cos^2\theta = z^2/r^2$. Let us take the radius of the cone-shaped microchannel as R_j at an arbitrary axial point of $z = z_j$, then $z_j = R_j/\tan\alpha$.

Figure 2 shows that the dimensionless radial velocity decreases with the increase of diverging angle. This is due to the fact that the cross-sectional area of the channel is increased, as the diverging angle increases. The velocity profiles for α less than 0.25 rad are almost the same. Note that $r^2 v_r$ is a function only of θ, and the diverging flow rate from the vertex leads to

$$q = \int_0^{2\pi}\int_0^{\alpha} r^2 v_r \sin\theta\, d\theta\, d\varphi = 2\pi r^2 v_r (1-\cos\alpha). \tag{4}$$

Taking the average velocity $\langle v_r\rangle$ into Eq. (4), a normalized flow function can be reasonably defined as $2(v_r/\langle v_r\rangle)(1-\cos\alpha)/\sin^2\alpha$. Figure 3 shows that the flow function increases in the center region of the channel with the increase of the diverging angle. In the wall region of the channel, in contrast, the flow function decreases with the increase of the diverging angle. Estimating from the potential distribution and velocity profile, the streaming current at the exit of the channel is much smaller than that in the entrance region. Hence, it is obvious that the streaming current induced in the pressure-driven flow direction is almost developed at the entrance of the channel.

3. Electrostatic field and electrokinetic analysis

In order to consider the streaming current generated by the flow of the ions in electrolyte solution, both the electrical potential distribution and the charge density should be evaluated. The electrical potential distribution based on electric double layer theory is represented by the Debye length [20]. If the Debye length is the same as or larger than the hydraulic radius of the microchannel, further consideration should be given to the situation of Debye length overlap and complication of the electrostatic potential distribution in a microchannel.

3.1. Electrostatic field within a straight cylindrical microchannel

We properly consider a cone-shaped microchannel as an assemblage of uniformly charged cylindrical microchannels, as illustrated in Fig. 1. The electrostatic field in a unit straight cylindrical microchannel can be readily solved, where the radius is R_j and the electrostatic potential at the dielectric solid wall is ζ. We begin with a Poisson equation relating the electrostatic potential ψ and the charge density ρ_e at every point in the microchannel space. Assuming that the ion concentration follows the Boltzmann distribution leads to the well-known nonlinear P–B equation.

A linearized version of this equation for low surface potential corresponds to the Debye–Hückel (D–H) approximation, expressed as

$$\nabla^2\psi = \kappa^2 \sinh\left(\frac{Z_k e\psi}{k_B T}\right) \cong \kappa^2\psi \quad \text{for } \psi \leqslant \frac{k_B T}{Z_k e}, \tag{5}$$

where k_B is the Boltzmann constant, T the absolute temperature, and e the unit charge. With the concentration n_k and the valence Z_k of ion species k, the inverse Debye length κ is given by $(2n_k Z_k^2 e^2/\varepsilon k_B T)^{1/2}$ for symmetric 1:1 electrolyte system. For aqueous solutions at 25 °C, the ionic concentration of 1.0 mM corresponds to the Debye length of 9.7 nm.

From Eq. (5), the electrostatic potential ψ in the cylindrical microchannel is determined with the boundary conditions presented as

$$\psi = \zeta \quad \text{at } r = R_j, \tag{6a}$$

$$\frac{\partial \psi}{\partial r} = 0 \quad \text{at } r = 0. \tag{6b}$$

The electrostatic potential distribution is easily obtained as

$$\psi = \zeta \frac{I_0(\kappa r)}{I_0(\kappa R_j)}, \tag{7}$$

where I_0 is the modified Bessel function of the first kind of zeroth order. From the Poisson equation, the net volume charge density is then determined by

$$\rho_e = -\varepsilon \nabla^2 \psi = -\varepsilon \zeta \kappa^2 \frac{I_0(\kappa r)}{I_0(\kappa R_j)}. \tag{8}$$

Since small amounts of charge exist at the center of the microchannel, the ion transport seems to occur mostly near the microchannel wall.

3.2. Streaming current and conduction current in a cone-shaped microchannel

Once the electrolyte solution is forced through a microchannel under a pressure difference, the counterions in the mobile part of the electrical double layer are carried toward the downstream end. This causes the electric convection current (i.e., streaming current) I_s to flow in the direction of the solution flow, and the accumulation of ions sets up an electric field with the streaming potential. This field causes the conduction current I_c to flow back in the opposite direction. The net current I, flowing in the axial direction of the microchannel, is the summation of the streaming current and the conduction current. The conduction current equals the streaming current at steady state; therefore, the net current should be zero as

$$I \equiv I_s + I_c = I_s + I_{c,w} + I_{c,b} = 0, \tag{9}$$

where $I_{c,w}$ is the conduction current through a microchannel wall and $I_{c,b}$ is the conduction current through the bulk solution of the microchannel.

The streaming current I_s generated by the flow of the unbalanced ions in the mobile double layer region is defined by an integration of the multiplication of both the velocity profile and the net charge density. For an arbitrary axial position of z_j with a unit volume of the cylinder, the streaming current takes the form

$$I_{s,z_j} \equiv \int\limits_{V,\ \text{at } z=z_j} v \rho_e \, dV, \tag{10}$$

where the unit cylinder at $z = z_j$ has a radius of R_j. The axial velocity profile can be devised as follows:

$$v_z = v_r \cos\theta$$

$$= \frac{3q}{2\pi} \frac{1}{(1+2\cos\alpha)(1-\cos\alpha)^2} \frac{z}{(r'^2+z^2)^{3/2}} \times \left(\frac{z^2}{r'^2+z^2} - \cos^2\alpha \right). \tag{11}$$

By substituting Eqs. (11) and (8) into Eq. (10), the correspondent streaming current is calculated as

$$I_{s,z_j} = \int\limits_0^{R_j} 2\pi r' v(r', z_j) \rho_e \, dr' = -3\varepsilon\zeta\kappa^2 q \Gamma, \tag{12}$$

where

$$\Gamma = \int\limits_0^{R_j} \frac{r'}{(1+2\cos\alpha)(1-\cos\alpha)^2} \frac{z_j}{(r'^2+z_j^2)^{3/2}} \times \left(\frac{z_j^2}{r'^2+z_j^2} - \cos^2\alpha \right) \frac{I_0(\kappa r')}{I_0(\kappa R_j)} dr'. \tag{13}$$

The average streaming current should be estimated because the streaming current varies with respect to the positions of r' as well as z. The individual streaming currents at each positions of axial direction are calculated, which may yield the following expression

$$I_s = \langle I_{s,z_j} \rangle = -3\varepsilon\zeta\kappa^2 q \langle \Gamma \rangle. \tag{14}$$

Although the electroosmotic flow induced by streaming potential in the cone-shaped channel is possibly occurred, it is not taken into account here to simplify the equation of the fluid motion. This assumption can be guaranteed for the case of lower surface potential (cf. D–H approximation) because the effect of electrostatic potential on the velocity profile is almost negligible.

As described above, the conduction current induced by the streaming potential difference ΔE consists of the bulk conduction current $I_{c,b}$ and the surface conduction current $I_{c,w}$ [21]. The bulk conduction current $I_{c,b}$ is calculated as follows. In the cone-shaped microchannel, we can reasonably consider a serially connected electrical resistance that is inversely proportional to the cross-sectional area of the unit cylinder. The resistance for the unit volume of cylinder with radius of R_j is thought of as an inverse quantity of the product of the bulk conductivity λ_0 per unit axial length and the cross-sectional area of the cylinder, or $(\Delta z/\lambda_0)(1/\pi R_j^2)$. Therefore, the relationship between the bulk conduction current and the streaming potential difference can be written as

$$\Delta E \equiv \sum_j \Delta E_j = I_{c,b} \frac{\Delta z}{\lambda_0} \sum_{R_i}^{R_f} \frac{1}{\pi R_j^2} \approx \frac{I_{c,b}}{\lambda_0} \int\limits_{z_i}^{z_f} \frac{dz_j}{\pi R_j^2}, \tag{15}$$

where R_i and R_f are the inlet and outlet radii of the microchannel, respectively. Applying the relationship between

R_j and z_j (i.e., $R_j = z_j \tan\alpha$) yields

$$\int_{z_i}^{z_f} \frac{dz_j}{\pi R_j^2} = \frac{1}{\pi} \frac{z_f - z_i}{z_i z_f \tan^2\alpha}. \tag{16}$$

Substituting Eq. (16) into Eq. (15) gives the bulk conduction current $I_{c,b}$, written as

$$I_{c,b} = \Delta E \pi \lambda_0 \frac{z_i z_f \tan^2\alpha}{z_f - z_i}. \tag{17}$$

Next, the surface conduction current $I_{c,w}$ is given by

$$I_{c,w} = \Delta E \lambda_{s,c} W_a, \tag{18}$$

where $\lambda_{s,c}$ is the surface conductivity per unit area. The surface area of the cone-shaped microchannel W_a can be provided as

$$W_a = \pi \left\{ R_f \sqrt{R_f^2 + \left(z_f + \frac{R_i}{\tan\alpha} \right)^2} - R_i \sqrt{R_i^2 + \left(\frac{R_i}{\tan\alpha} \right)^2} \right\}. \tag{19}$$

4. Helmholtz–Smoluchowski equation for diverging flow

A substitution of Eqs. (14), (17), and (18) into Eq. (9) gives the relation between the streaming current and the conduction current. However, the surface conduction current $I_{c,w}$, can be neglected, because the surface conductivity is quite smaller than the bulk conductivity of the electrolyte solution (e.g., the value of λ_s/λ_0 is an order of 10^{-7} for aqueous solution through the glass surface). Then, combining both Eqs. (14) and (17) yields

$$\frac{\Delta E}{q} = \frac{3\varepsilon\zeta\kappa^2}{\pi\lambda_0} \frac{(z_f - z_i)}{z_i z_f \tan^2\alpha} \langle \Gamma \rangle. \tag{20}$$

The pressure gradient to the axial direction varies at every position in the cone-shaped microchannel. Henceforth, the pressure difference between the microchannel ends is calculated on the basis of the pressure distribution equation given as [18]

$$P = P_\infty - \frac{\mu q}{\pi r^3} \frac{1 - 3\cos^2\theta}{(1 + 2\cos\alpha)(1 - \cos\alpha)^2}. \tag{21}$$

For the symmetric axis of the microchannel (i.e., $\theta = 0$), the inlet and outlet pressures are given as $P^i_{\theta=0}$ and $P^f_{\theta=0}$, respectively. The pressure difference at the symmetric axis is then expressed as

$$\Delta P_{\theta=0} = P^f_{\theta=0} - P^i_{\theta=0} = \frac{\mu q}{\pi} \left(\frac{1}{r_f^3} - \frac{1}{r_i^3} \right) \frac{2}{(1 + 2\cos\alpha)(1 - \cos\alpha)^2}, \tag{22}$$

where r_i and r_f indicate the radial lengths at inlet and outlet points, respectively.

From the calculation of Eq. (21), we know that the pressure difference at the symmetric axis is nearly equivalent to the average pressure difference between inlet and outlet positions of the cone-shaped microchannel. Based on this emphasis, the average pressure difference can be considered as the pressure difference at the symmetric axis,

$$\Delta P \approx \Delta P_{\theta=0}. \tag{23}$$

From Eq. (23), we can develop the relationship between the volumetric flow rate and the pressure difference in cylindrical coordinates, so that

$$q = \frac{\pi \Delta P}{2\mu} q', \tag{24}$$

where

$$q' = (1 - 2\cos\alpha)(1 - \cos\alpha)^2 \times \frac{[(z_i^2 + z_i^2 \tan^2\alpha)(z_f^2 + z_f^2 \tan^2\alpha)]^{3/2}}{(z_i^2 + z_i^2 \tan^2\alpha)^{3/2} - (z_f^2 + z_f^2 \tan^2\alpha)^{3/2}}. \tag{25}$$

Substituting Eq. (24) into Eq. (20) finally gives the correct H–S equation for cone-shaped channels, as

$$\frac{\Delta E}{\Delta P} = \frac{\varepsilon\zeta}{\mu\lambda_0} \left[\frac{3\kappa^2 (z_f - z_i) q' \langle \Gamma \rangle}{2(z_i z_f \tan^2\alpha)} \right] = \left. \frac{\Delta E}{\Delta P} \right|_{\text{H–S}} \left[\frac{3\kappa^2 (z_f - z_i) q' \langle \Gamma \rangle}{2(z_i z_f \tan^2\alpha)} \right]. \tag{26}$$

Equation (26) allows us to understand that the effects of channel geometry as well as streaming current upon the correct H–S equation are reflected in the correction ratio, or $(\Delta E/\Delta P)/(\Delta E/\Delta P)_{\text{H–S}}$. Both the diverging angle and the channel length determine the geometric effect, whereas the Debye length is pertinent to the electrostatic property of the channel.

In the computation of Eq. (26), the number of unit cylinders should be chosen successfully. We found that numerical integration with 25 points is sufficient to yield accurate results. Figure 4 shows that the correction ratio $(\Delta E/\Delta P)/(\Delta E/\Delta P)_{\text{H–S}}$ decreases with increasing diverging angle, from which the zeta potential of the cone-shaped divergent channel is evaluated as a smaller value compared to a cylindrical channel. At a given diverging angle, the correction ratio decreases monotonically with a decreased ratio of channel inlet radius to Debye length, or κR_i. This tendency can be explained by the overlapping of Debye length, and a similar trend is found in the literature studied on the cylindrical channel. Figure 5 shows that, at the given value of κR_i, the correction ratio decreases as the channel length z_f increases. The radius of channel outlet increases according to the increase of channel length, which results in a decreased axial velocity due to a diverging flow effect. As a result, the zeta potential of the channel becomes smaller.

As shown in Fig. 6, as the diverging angle approaches zero, the correction ratio estimated from the correct H–S

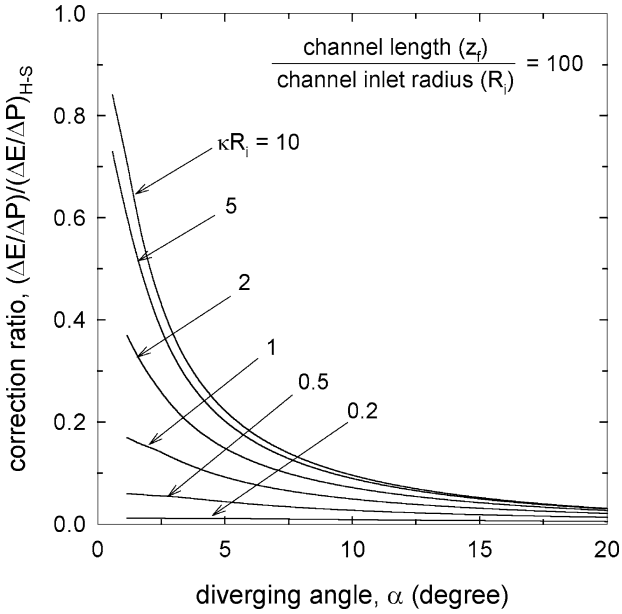

Fig. 4. The variation of the correction ratio at various κR_i as a function of the diverging angle α.

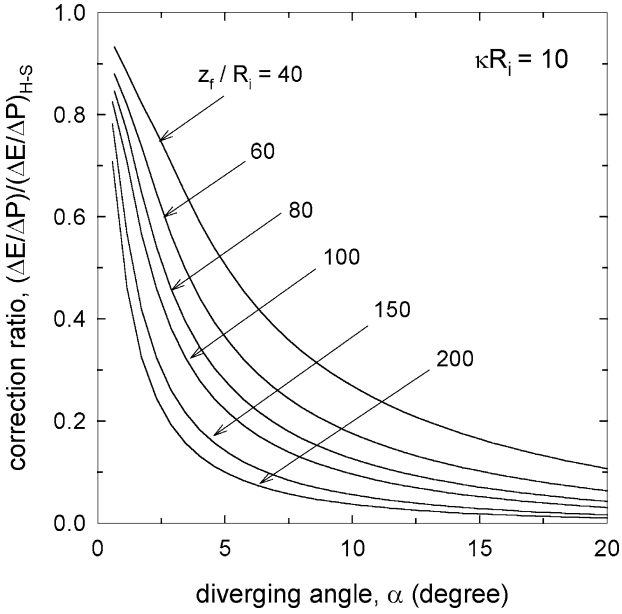

Fig. 5. The variation of the correction ratio at various z_f/R_i as a function of the diverging angle α.

equation converges asymptotically to those of the straight cylindrical channel considered by Rice and Whitehead [2] as well as Bowen and Cao [11]. As the diverging angle increases, the correction ratio evidently decreases and its dependency on κR_i deviates from the case of the cylindrical channel. Figure 6 shows that, once the zeta potential of the cone-shaped channel needs to be estimated, both the geometric parameters and the electrostatic properties should be considered carefully. Finally, it is worth pointing out that experimental results can be provided to illustrate the implication of the present correct H–S equation for the electrokinetic characterization of relevant microchannels, which is a good subject of further study.

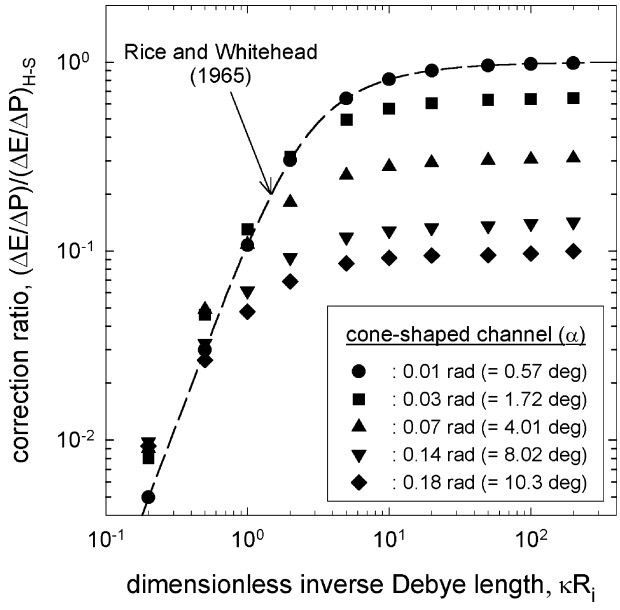

Fig. 6. The variation of the correction ratio at various diverging angles α as a function of κR_i. The previous result [2] is also provided for comparison, with the parameter β $(= \varepsilon^2\psi_s^2\kappa^2/16\pi^2\mu\lambda_0)$ taken as 0.225.

5. Conclusions

In this study, electrokinetic effects in the cone-shaped divergent channel were analyzed, and the corresponding correct H–S equation was derived. From this H–S equation, it can be inferred that both the geometry of the divergent channel and the Debye length affect the determination of the electrokinetic zeta potential. We found that the increase of diverging angle reduces the correction ratio, which means smaller zeta potential is generated as the diverging angle increases in the cone-shaped channel. The correction ratio was also decreased with decreasing dimensionless inverse Debye length, due to the overlapping of the Debye length inside the channel.

The correct H–S equation agrees well with the previously proposed result derived from the straight cylindrical channel; however, a growth of deviation is shown as the diverging angle increases. Obviously, it is important to take into account the effects of the geometry and the Debye length in estimating a rigorous zeta potential of the cone-shaped channel.

Acknowledgment

This work was supported by the Basic Research Fund (Grant R01-2001-000-00411-0) from the Korea Science and Engineering Foundations (KOSEF) provided to M.-S.C.

Appendix A. Nomenclature

E	streaming potential (V)
e	elementary charge (Coul)
$I_{c,b}$	conduction current flowing through the electrolyte solution in the channel (Amp)
$I_{c,w}$	conduction current flowing through the channel wall (Amp)
I_s	streaming current (Amp)
I_0	modified Bessel function of the first kind of zeroth order (–)
k_B	Boltzmann constant (J/K)
n_k	concentration of ion species k ($\mathrm{mol/m^3}$)
P	pressure ($\mathrm{N/m^2}$)
q	volumetric flow rate flowing through the cone-shaped microchannel ($\mathrm{m^3/s}$)
q'	factor defined in Eq. (25) (–)
R	channel radius (m)
r	radial coordinate in spherical coordinates (–)
r'	radial coordinate in cylindrical coordinates (–)
T	absolute temperature (K)
V	unit volume ($\mathrm{m^3}$)
v	fluid velocity (m/s)
W_a	surface area of channel wall ($\mathrm{m^2}$)
Z_k	valence of ion species k (–)
z	axial coordinate in cylindrical coordinates (–)

Greek symbols

α	diverging angle (deg)
Γ	factor defined in Eq. (13) (–)
ε	dielectric constant (Coul/V m)
ζ	zeta potential (V)
θ	polar angle (deg)
κ	inverse Debye length (1/m)
λ_0	electrolyte conductivity ($1/\Omega\,\mathrm{m}$)
λ_s	specific surface conductivity (S)
$\lambda_{s,c}$	surface conductivity per channel area ($1/\Omega\,\mathrm{m^2}$)
μ	viscosity of electrolyte solution (kg/m s)
ρ_e	net volume charge density ($\mathrm{Coul/m^3}$)
Φ	stream function (–)
φ	azimuthal angle (deg)
ψ	electrostatic potential (V)

Subscripts

f	channel outlet
i	channel inlet
j	arbitrary unit channel

References

[1] M. von Smoluchowski, Z. Phys. Chem. 93 (1918) 129.
[2] C.L. Rice, R. Whitehead, J. Phys. Chem. 69 (1965) 4017.
[3] S. Levine, J.R. Marriott, G. Neale, N. Epstein, J. Colloid Interface Sci. 52 (1975) 136.
[4] M. Nyström, M. Lindström, E. Matthiasson, Colloids Surf. 36 (1989) 297.
[5] C. Causserand, M. Nyström, P. Aimar, J. Membrane Sci. 88 (1994) 211.
[6] K.J. Kim, A.G. Fane, M. Nyström, A. Pihlajamäki, W.R. Bowen, H. Mukhtar, J. Membrane Sci. 116 (1996) 149.
[7] L. Ricq, A. Pierre, J.-C. Reggiani, J. Pagetti, A. Foissy, Colloids Surf. A Physicochem. Eng. Aspects 138 (1998) 301.
[8] D. Möckel, E. Staude, M. Dal-Cin, K. Darcovich, M. Guiver, J. Membrane Sci. 145 (1998) 211.
[9] A. Szymczyk, B. Aoubiza, P. Fievet, J. Pagetti, J. Colloid Interface Sci. 216 (1999) 285.
[10] M.-S. Chun, G.-Y. Chung, J.-J. Kim, J. Membrane Sci. 193 (2001) 97.
[11] W.R. Bowen, X. Cao, J. Membrane Sci. 140 (1998) 267.
[12] A. Szymczyk, C. Labbez, P. Fievet, B. Aoubiza, C. Simon, AIChE J. 47 (2001) 2349.
[13] J.L. Anderson, W.-H. Koh, J. Colloid Interface Sci. 59 (1977) 149.
[14] C. Yang, D. Li, J. Colloid Interface Sci. 194 (1997) 95.
[15] G.E. Karniadakis, A. Beskok, Micro Flows: Fundamentals and Simulation, Springer-Verlag, New York, 2002.
[16] W.A. Lyon, S. Nie, Anal. Chem. 69 (1997) 3400.
[17] R.C. Furneaux, W.R. Rigby, A.P. Davidson, Nature 337 (1989) 147.
[18] J. Happel, H. Brenner, Low Reynolds Number Hydrodynamics: With Special Applications to Particulate Media, Martinus Nijhoff, Dordrecht, 1983.
[19] M.-S. Chun, J.-J. Kim, Membrane J. 7 (1997) 142.
[20] R.J. Hunter, Zeta Potential in Colloid Science: Principles and Applications, Academic Press, London, 1981.
[21] P. Bouriat, P. Saulnier, P. Brochette, A. Graciaa, J. Lachaise, J. Colloid Interface Sci. 209 (1999) 445.